

Weilie Zhou
Zhong Lin Wang *Editors*

Three-Dimensional Nanoarchitectures

Designing Next-Generation Devices

 Springer

Three-Dimensional Nanoarchitectures

Weilie Zhou · Zhong Lin Wang
Editors

Three-Dimensional Nanoarchitectures

Designing Next-Generation Devices

 Springer

Editors

Weilie Zhou
Advanced Materials Research Institute
University of New Orleans
2000 Lakeshore Drive
New Orleans, LA 70148, USA
wzhou@uno.edu

Zhong Lin Wang
School of Materials Science and
Engineering
Georgia Institute of Technology
771 Ferst Drive, N.W.
Atlanta, GA 30332-0245, USA
zhong.wang@mse.gatech.edu

ISBN 978-1-4419-9821-7

e-ISBN 978-1-4419-9822-4

DOI 10.1007/978-1-4419-9822-4

Springer New York Dordrecht Heidelberg London

Library of Congress Control Number: 2011930518

© Springer Science+Business Media, LLC outside the People's Republic of China, © Weilie Zhou and Zhong Lin Wang in the People's Republic of China 2011

All rights reserved. This work may not be translated or copied in whole or in part without the written permission of the publisher (Springer Science+Business Media, LLC, 233 Spring Street, New York, NY 10013, USA), except for brief excerpts in connection with reviews or scholarly analysis. Use in connection with any form of information storage and retrieval, electronic adaptation, computer software, or by similar or dissimilar methodology now known or hereafter developed is forbidden.

The use in this publication of trade names, trademarks, service marks, and similar terms, even if they are not identified as such, is not to be taken as an expression of opinion as to whether or not they are subject to proprietary rights.

Printed on acid-free paper

Springer is part of Springer Science+Business Media (www.springer.com)

Contents

1 Building 3D Nanostructured Devices by Self-Assembly	1
Steve Hu, Jeong-Hyun Cho, and David H. Gracias	
1.1 The Pressing Need for 3D Patterned Nanofabrication	1
1.2 Self-Assembly Using Molecular Linkages	3
1.2.1 Three-Dimensional Self-Assembly Using Protein Linkages	4
1.2.2 Three-Dimensional Self-Assembly with DNA Linkages	6
1.3 Three-Dimensional Self-Assembly Using Physical Forces	10
1.4 Three-Dimensional Patterned Nanofabrication by Curving and Bending Nanostructures	12
1.4.1 Curving Hingeless Nanostructures Using Stress	13
1.4.2 Three-Dimensional Nanofabrication by Bending Hinged Panels to Create Patterned Polyhedral Nanoparticles	20
1.5 Conclusions	22
References	23
2 Bio-inspired 3D Nanoarchitectures	29
Jian Shi and Xudong Wang	
2.1 Introduction	29
2.2 Historical Perspective	31
2.3 Bio-inspired Nanophotonics	31
2.3.1 Photonic Crystals	31
2.3.2 Color Mine in Nature	34
2.3.3 Natural Photonic Crystals	35
2.3.3.1 Spine of Sea Mouse	35
2.3.3.2 Diatom	37
2.3.3.3 Butterfly Wings	37
2.3.3.4 Beetles	40
2.3.3.5 Weevil	43
2.3.4 Other Natural Photonics	43
2.3.4.1 Brittle Star	43
2.3.4.2 Glass Sponge	45

2.4	Bio-inspired Fabrication of Nanostructures	47
2.4.1	Biom mineralization	47
2.4.2	Biological Fine Structure Duplication	48
2.4.2.1	Replication by Surface Coating	49
2.4.2.2	Replication by Atom Exchange	52
2.5	Bio-inspired Functionality	54
2.6	Conclusion	56
	References	57
3	Building 3D Micro- and Nanostructures Through Nanoimprint . .	59
	Xing Cheng	
3.1	Introduction to 3D Structure Fabrication Through Nanoimprint .	59
3.2	Overview of Nanoimprint Lithography	60
3.2.1	Fundamentals of Nanoimprint Lithography	60
3.2.2	Materials for Nanoimprint Lithography	61
3.3	Building 3D Nanostructures by Nanoimprint	63
3.3.1	Direct Patterning of 3D Structures in One Step	63
3.3.1.1	Replicating 3D Polymer Structures from 3D Templates	63
3.3.1.2	Applications of 3D Polymer Structures by One-Step Nanoimprint	65
	Dual Damascene Structure for Back-End Processing of Microelectronic Circuit Chips	66
	Advanced Optical Components Based on 3D Polymer Structures	67
3.3.2	Building 3D Nanostructures by Transfer Bonding and Sequential Layer Stacking	70
3.3.2.1	Principles of Transfer Bonding and Sequential Layer Stacking	70
3.3.2.2	3D Structures Built by Transfer Bonding and Sequential Layer Stacking	72
3.3.2.3	Defect Modes and Process Yield of Transfer Bonding and Sequential Layer Stacking	80
3.3.3	Building 3D Nanostructures by Two Consecutive Nanoimprints	82
3.4	Summary and Future Outlook	82
	References	84
4	Electrochemical Growth of Nanostructured Materials	89
	Jin-Hee Lim and John B. Wiley	
4.1	Magnetic Nanomaterials	90
4.2	Semiconductor Nanostructures	93
4.3	Thermoelectric Nanomaterials	95
4.4	Conducting Polymer Nanostructures	96

4.5	Nanotube and Core–Shell Nanostructures	98
4.6	Porous Au Nanowires	99
4.7	Modification of Nanowires	102
4.8	Functionalization of Nanowires	104
4.9	Nanostructure Arrays on Substrates	106
4.10	Patterning of Nanowires	107
	References	111
5	Three-Dimensional Micro/Nanomaterials Generated by Fiber-Drawing Nanomanufacturing	117
	Zeyu Ma, Yan Hong, Shujiang Ding, Minghui Zhang, Mainul Hossain, and Ming Su	
5.1	Introduction	117
5.2	Fiber Draw Tower	117
5.3	Materials Selections	119
5.4	Drawing Process	119
5.5	Size Design	120
5.6	Three-Dimensional Assembling	122
5.7	Metallic Nanowires	122
5.8	Semiconductor Nanowires	123
5.9	Glass Microchannel Array	125
5.10	Differential Etching of Glasses	125
5.11	Glass Microspike Array	126
5.12	Hybrid Glass Membranes	128
5.13	Textured Structure of Encapsulated Paraffin Wax Microfiber	130
5.14	Conclusions	131
	References	131
6	One-Dimensional Metal Oxide Nanostructures for Photoelectrochemical Hydrogen Generation	133
	Yat Li	
6.1	Introduction	133
6.1.1	Photoelectrochemical Hydrogen Generation	133
6.1.2	Challenges in Metal Oxide-Based PEC Hydrogen Generation	135
6.1.3	One-Dimensional Nanomaterials for Photoelectrodes	136
6.2	Pristine Metal Oxide Nanowire/Nanotube-Arrayed Photoelectrodes	138
6.2.1	Nanowire-Arrayed Photoelectrodes	138
6.2.1.1	Hematite (α -Fe ₂ O ₃)	138
6.2.1.2	Titanium Oxide (TiO ₂) and Zinc Oxide (ZnO)	139
6.2.1.3	Tungsten Trioxide (WO ₃)	142
6.2.2	Nanotube-Arrayed Photoelectrodes	143

6.3	Element-Doped Metal Oxide 1D Nanostructures	146
6.3.1	TiO ₂ Nanostructures	146
6.3.2	ZnO Nanostructures	149
6.3.3	Hematite (α -Fe ₂ O ₃) Nanostructures	149
6.4	Quantum Dot Sensitizations	152
6.4.1	Background	152
6.4.2	Quantum Dot-Sensitized ZnO Nanowires	153
6.4.3	Quantum Dot-Cosensitized Nanowires	154
6.4.4	Double-Sided Quantum Dot Sensitization	155
6.5	Synergistic Effect of Quantum Dot Sensitization and Elemental Doping	158
6.6	Concluding Remarks	160
	References	162
7	Helical Nanostructures: Synthesis and Potential Applications . . .	167
	Pu-Xian Gao and Gang Liu	
7.1	Introduction	167
7.2	Semiconductor Nanohelices	168
7.2.1	ZnO Nanohelices	168
7.2.1.1	Superlattice-Structured ZnO Nanohelices . .	168
7.2.1.2	Superelasticity, Nanobuckling, and Nonlinear Electronic Transport of Superlattice-Structured ZnO Nanohelices Superelasticity of Superlattice- Structured ZnO Nanohelix	171
	Nanobuckling and Fracture of Superlattice-Structured ZnO Nanohelix	172
	Nonlinear Electronic Transport of Superlattice-Structured ZnO Nanohelix	174
7.2.1.3	Other ZnO Nanohelices	176
7.2.2	SiO ₂ Nanohelices	178
7.2.3	CdS Nanohelices	183
7.2.4	InP Nanohelices	188
7.2.5	Ga ₂ O ₃ Nanohelices	190
7.3	Carbon-Related Nanohelices	191
7.3.1	Helical Carbon Nanoribbon/Nanocoil	192
7.3.2	Helical Carbon Nanotube	194
7.3.3	Tungsten-Containing Carbon (WC) Nanospring	195
7.4	Other Nanohelices	197
7.4.1	Helical SiC/SiO ₂ Core-Shell Nanowires and Si ₃ N ₄ Microcoils	197
7.4.2	MgB ₂ Nanohelices	198
7.4.3	Si Spirals	199
7.5	Potential Applications	201

7.6	Summary	202
	References	202
8	Hierarchical 3D Nanostructure Organization for Next-Generation Devices	205
	Eric N. Dattoli and Wei Lu	
8.1	Introduction	205
8.2	Fluidic Flow-Assisted Assembly	206
	8.2.1 Drop-Drying	207
	8.2.2 Channel-Confined Fluidic Flow	208
	8.2.3 Blown Bubble Film Transfer	210
8.3	Nematic Liquid Crystal-Induced Assembly	212
8.4	Langmuir–Blodgett Assembly	213
8.5	Dielectrophoresis Assembly	215
8.6	Chemical Affinity and Electrostatic Interaction-Directed Assembly	219
8.7	Contact Transfer	221
	8.7.1 Shear-Assisted Contact Printing	221
	8.7.2 Stamp Transfer	224
8.8	Directed Growth	226
	8.8.1 Horizontal Growth	226
	8.8.2 Vertical Growth	228
8.9	Device Applications	230
	8.9.1 Thin-Film Transistors	230
	8.9.1.1 Performance Considerations for NW- or NT-Based TFTs	230
	8.9.1.2 Transparent Nanowire-Based TFTs	233
	8.9.1.3 CNT-Based TFTs	235
	8.9.2 3D Multilayer Device Structures	237
	8.9.3 Sensors	240
	8.9.4 Vertical Nanowire Field-Effect Transistors (FETs)	242
8.10	Conclusion	243
	References	243
9	Strain-Induced, Self Rolled-Up Semiconductor Microtube Resonators: A New Architecture for Photonic Device Applications	249
	Xin Miao, Ik Su Chun, and Xiuling Li	
9.1	Introduction	249
9.2	Formation Process	250
9.3	Photonic Applications of Rolled-Up Semiconductor Tubes	252
	9.3.1 Spontaneous Emission from Quantum Well Microtubes: Intensity Enhancement and Energy Shift	252
	9.3.2 Optical Resonance Modes in Rolled-Up Microtube Ring Cavity	254
	9.3.3 Optically Pumped Lasing from Rolled-Up Microtube Ring Cavity	256
	References	258

10	Carbon Nanotube Arrays: Synthesis, Properties, and Applications	261
	Suman Neupane and Wenzhi Li	
10.1	Introduction	261
10.2	Carbon Nanotube Synthesis	262
10.2.1	Arc Discharge	262
10.2.2	Laser Ablation	262
10.2.3	Electrochemical Synthesis	263
10.2.4	Diffusion Flame Synthesis	264
10.2.5	Chemical Vapor Deposition	264
10.3	Carbon Nanotube Arrays	265
10.3.1	CNTA Synthesis Using Patterned Catalyst Arrays	266
10.3.1.1	Pulsed Laser Deposition	266
10.3.1.2	Anodic Aluminum Oxide (AAO) Templates	266
10.3.1.3	Reverse Micelle Method	266
10.3.1.4	Photolithography	267
10.3.1.5	Electrochemical Etching	268
10.3.1.6	Sputtering	268
10.3.1.7	Nanosphere Lithography	268
10.3.1.8	Sol–Gel Method	269
10.3.2	CNTA Synthesis by Other Methods	269
10.3.3	Horizontal Arrays of CNTs	270
10.4	Mechanical Properties	270
10.5	Thermal Properties	271
10.6	Electrical Properties	273
10.7	Applications of CNTs and CNTAs	276
10.7.1	Hydrogen Storage	276
10.7.2	CNTs as Sensors	278
10.7.3	CNTs for Battery and Supercapacitor Applications	279
10.7.4	CNTs for Photovoltaic Device	279
10.8	Conclusions	280
	References	281
11	Molecular Rotors Observed by Scanning Tunneling Microscopy	287
	Ye-Liang Wang, Qi Liu, Hai-Gang Zhang, Hai-Ming Guo, and Hong-Jun Gao	
11.1	Introduction	287
11.2	Solution-Based and Surface-Mounted Molecular Machines	289
11.3	Single Molecular Rotors at Surfaces	290
11.3.1	A Monomolecular Rotor in Supramolecular Network	290
11.3.2	Gear-Like Rotation of Molecular Rotor Along the Edge of the Molecular Island	292
11.3.3	Thermal-Driven Rotation on Reconstructed Surface Template	292
11.3.4	STM-Driven Rotation on Reconstructed Surface Template	301

11.3.5	Molecular Rotors with Variable Rotation Radii	303
11.3.6	Rolling Motion of a Single Molecule at the Surface	305
11.4	Array of Molecular Motors at Surfaces	308
11.5	Outlook	310
11.6	Conclusion	311
	References	311
12	Nanophotonic Devices Based on ZnO Nanowires	317
	Qing Yang, Limin Tong, and Zhong Lin Wang	
12.1	Introduction	317
12.2	Pure Optical Devices Based on ZnO NWs	318
12.2.1	ZnO NW Subwavelength Waveguides and Their Applications	318
12.2.2	Optically Pumped Lasers in ZnO NWs	322
12.2.3	Nonlinear Optical Devices Based on ZnO NWs	330
12.3	Optoelectronic Devices Based ZnO NWs	333
12.3.1	ZnO NW Ultra-sensitive UV and Infrared PDs	333
12.3.2	Dye-Sensitized Solar Cells Based on ZnO NWs	339
12.3.3	Single ZnO NW and NW Array Light-Emitting Diodes	345
12.3.4	Electrically Pumped Random Lasing from ZnO Nanorod Arrays	350
12.4	Piezo-phototronic Devices Based on ZnO NWs	352
12.4.1	Optimizing the Power Output of a ZnO Photocell by Piezopotential	353
12.4.2	Enhancing Sensitivity of a Single ZnO Micro-/NW Photodetector by Piezo-phototronic Effect	354
12.5	Conclusions	356
	References	356
13	Nanostructured Light Management for Advanced Photovoltaics	363
	Jia Zhu, Zongfu Yu, Sangmoo Jeong, Ching-Mei Hsu, Shanui Fan, and Yi Cui	
13.1	Introduction	363
13.2	Fabrication of Nanowire and Nanocone Arrays	365
13.2.1	Method	366
13.2.2	Shape Control: Nanowires and Nanocones	366
13.2.3	Diameter and Spacing Control	368
13.2.4	Large-Scale Process	368
13.3	Photon Management: Antireflection	372
13.3.1	Nanowires	372
13.3.2	Nanocones	374
13.4	Photon Management: Absorption Enhancement	376
13.4.1	Different Mechanisms	376
13.4.2	Nanodome Structures	378
13.5	Solar Cell Performance	383

13.6 Fundamental Limit of Light Trapping in Nanophotonics 384

13.7 Summary and Outlook 388

References 389

14 Highly Sensitive and Selective Gas Detection by 3D Metal Oxide Nanoarchitectures 391

Jiajun Chen, Kai Wang, Baobao Cao, and Weilie Zhou

14.1 Introduction 391

14.2 Highly Sensitive Gas Detection by Stand-alone 3D Nanosensors 394

 14.2.1 Metal Oxide Nanowire/Nanotube Array Gas Sensors . 395

 14.2.1.1 Nanowire Arrays 395

 14.2.1.2 Nanotube Arrays 399

 14.2.2 Gas Sensors Based on Opal and Inverted Opal Nanostructures 401

14.3 Sensor Arrays Based on 3D Nanostructured Gas Sensors 403

14.4 Conclusion Remarks 408

References 409

15 Quantum Dot-Sensitized, Three-Dimensional Nanostructures for Photovoltaic Applications 413

Jun Wang, Xukai Xin, Daniel Vennerberg, and Zhiqun Lin

15.1 Introduction 413

15.2 Quantum Dot-Sensitized Solar Cells 415

 15.2.1 Overview 415

 15.2.2 Synthesis of Quantum Dots and Surface Functionalization 415

 15.2.3 Quantum Dot-Sensitized Nanoparticle Films 419

 15.2.4 Quantum Dot-Sensitized Nanowire Arrays 426

 15.2.5 Quantum Dot-Sensitized Nanotube Arrays 428

 15.2.6 Investigation of Charge Injection in Quantum Dot-Sensitized Solar Cells 432

 15.2.6.1 Generation of Excited Electrons 432

 15.2.6.2 Recombination and Transportation of Excited Electrons 434

15.3 Outlook 438

References 439

16 Three-Dimensional Photovoltaic Devices Based on Vertically Aligned Nanowire Array 447

Kai Wang, Jiajun Chen, Satish Chandra Rai, and Weilie Zhou

16.1 Introduction 447

16.2 Photovoltaic Devices Based on Nanowire Array Integrated with the Substrate 448

16.3 Photovoltaic Devices Based on Nanowire Array with Axial Junctions 451

16.4	Photovoltaic Devices Based on Nanowire Array Embedded in Thin Film	452
16.5	Photovoltaic Devices Based on Nanowire Array with Core–Shell Structure	453
16.5.1	p–n Core–Shell Homojunction Photovoltaic Devices	453
16.5.2	Type II Core–Shell Heterojunction Photovoltaic Devices	456
16.5.2.1	Synthesis of ZnO/ZnSe and ZnO/ZnS Core–Shell Nanowire Array	457
16.5.2.2	Structural and Optical Properties of ZnO/ZnSe Core–Shell Nanowire Array	458
16.5.2.3	Photoresponse of ZnO/ZnSe Nanowire Array	461
16.5.2.4	Morphologies, Structure and Optical Properties of ZnO/ZnS Nanowire Array	462
16.5.2.5	Photovoltaic Effect of ZnO/ZnS Nanowire Array	465
16.6	Summary and Perspectives	469
	References	471
17	Supercapacitors Based on 3D Nanostructured Electrodes	477
	Hao Zhang, Gaoping Cao, and Yusheng Yang	
17.1	Supercapacitors	478
17.2	Electrochemical Double Layer Capacitors Based on 3D Nanostructured Electrodes	479
17.2.1	Electrodes Based on Activated Carbons and Activated Carbon Fibers: Powdered Carbons with Disordered Pore Structures	480
17.2.2	Electrodes Based on Carbon Foams, Carbon Aerogels, and Other Monolithic Carbon: Monolithic Carbon with Disordered Micropores	483
17.2.3	Electrodes Based on Template Carbons, Graphene, Carbide-Derived Carbons, and Hierarchical Porous Carbons: Powdered Carbons with High Mesopore Ratios or Reasonable PSD	486
17.2.4	Electrodes Based on Carbon Nanotubes: Monolithic Carbons with Developed Mesoporous Structures	492
17.3	Pseudo-capacitors Based on 3D Nanostructured Electrodes	497
17.3.1	Nanostructured Metal Oxide Electrode Materials	498
17.3.2	Nanostructured Conducting Polymer Electrode Materials	500
17.4	Hybrid Capacitors Based on 3D Nanostructured Electrodes	502

17.4.1	Nanostructured Electrodes Based on Metal Oxides/Carbon Composite	504
17.4.2	Nanostructured Electrodes Based on Polymers/Carbon Composites	508
17.5	Conclusions and Perspectives	513
	References	514
18	Aligned Ni-Coated Single-Walled Carbon Nanotubes Under Magnetic Field for Coolant Applications	523
	Haiping Hong, Mark Horton, and G.P. Peterson	
18.1	Introduction	523
18.2	Experiment	524
18.3	Results and Discussion	525
18.3.1	Thermal Conductivity of Nanofluids Containing Ni-Coated Nanotubes	525
18.3.2	Evidence of Magnetic Alignment of Ni-Coated Nanotubes	529
18.4	Conclusion	533
	References	534
Index	535

Contributors

Baobao Cao Advanced Materials Research Institute, University of New Orleans, New Orleans, LA 70148, USA, bcao1@uno.edu

Gaoping Cao Research Institute of Chemical Defense, Beijing 100191, China, caogaoping@tom.com

Jiajun Chen Advanced Materials Research Institute, University of New Orleans, New Orleans, LA 70148, USA, jchen2@uno.edu

Xing Cheng Department of Electrical and Computer Engineering, Texas A&M University, College Station, TX 77843-3128, USA, chengx@ece.tamu.edu

Jeong-Hyun Cho Department of Chemical and Biomolecular Engineering, The Johns Hopkins University, Baltimore, MD 21218, USA, itrustyou@gmail.com

Ik Su Chun Micro and Nanotechnology Laboratory, Department of Electrical and Computer Engineering, University of Illinois, Urbana, IL 61801, USA, ichun2@illinois.edu

Yi Cui Department of Materials Science and Engineering, Stanford University, Stanford, CA 94305, USA, yicui@stanford.edu

Eric N. Dattoli Department of Electrical Engineering and Computer Science, University of Michigan, Ann Arbor, MI 48109-2122, USA, edattoli1@gmail.com

Shujiang Ding NanoScience Technology Center, University of Central Florida, Orlando, FL 32826, USA, sjding@mail.ucf.edu

Shanui Fan Department of Electrical Engineering, Stanford University, Stanford, CA 94305, USA, shanhui.fan@stanford.edu

Hong-Jun Gao Institute of Physics, Chinese Academy of Sciences, Beijing 100190, China, hjgao@iphy.ac.cn

Pu-Xian Gao Department of Chemical, Materials and Biomolecular Engineering and Institute of Materials Science, University of Connecticut, Storrs, CT 06269-3136, USA, puxian.gao@ims.uconn.edu

David H. Gracias Department of Chemical and Biomolecular Engineering, The Johns Hopkins University, Baltimore, MD 21218, USA, dgracias@jhu.edu

Hai-Ming Guo Institute of Physics, Chinese Academy of Sciences, Beijing 100190, China, hmguo@iphy.ac.cn

Haiping Hong Department of Material and Metallurgical Engineering, South Dakota School of Mines and Technology, Rapid City, SD 57701, USA, haiping.hong@sdsmt.edu

Yan Hong NanoScience Technology Center, University of Central Florida, Orlando, FL 32826, USA; Department of Mechanical, Materials and Aerospace Engineering, University of Central Florida, Orlando, FL 32826, USA, yanhong@mail.ucf.edu

Mark Horton Department of Material and Metallurgical Engineering, South Dakota School of Mines and Technology, Rapid City, SD 57701, USA, mark.horton@mines.sdsmt.edu

Mainul Hossain School of Electrical Engineering and Computer Science, University of Central Florida, Orlando, FL 32826, USA, mainul@knights.ucf.edu

Ching-Mei Hsu Departments of Materials Science and Engineering and Electrical Engineering, Stanford University, Stanford, CA 94305, USA, chingmei1219@gmail.com

Steve Hu Department of Chemical and Biomolecular Engineering, The Johns Hopkins University, Baltimore, MD 21218, USA, shu5@buffalo.edu

Sangmoo Jeong Department of Electrical Engineering, Stanford University, Stanford, CA 94305, USA, popomoo@stanford.edu

Wenzhi Li Department of Physics, Florida International University, Miami, FL 33199, USA, liwenzhi@fiu.edu

Xiuling Li Micro and Nanotechnology Laboratory, Department of Electrical and Computer Engineering, University of Illinois, Urbana, IL 61801, USA, xiuling@illinois.edu

Yat Li Department of Chemistry and Biochemistry, University of California, Santa Cruz, CA 95064, USA, yatli@ucsc.edu

Jin-Hee Lim Department of Chemistry and Advanced Materials Research Institute, University of New Orleans, New Orleans, LA 70148, USA, jlim@uno.edu

Zhiqun Lin Department of Materials Science and Engineering, Iowa State University, Ames, IA 50011-2300, USA, zqlin@iastate.edu

Gang Liu Department of Chemical, Materials and Biomolecular Engineering, University of Connecticut, Storrs, CT 06269-3136, USA; Institute of Materials

Science, University of Connecticut, Storrs, CT 06269-3136, USA,
liugang.zzq@gmail.com

Qi Liu Institute of Physics, Chinese Academy of Sciences, Beijing 100190,
China, qliu@semi.ac.cn

Wei Lu Department of Electrical Engineering and Computer Science, University
of Michigan, Ann Arbor, MI 48109-2122, USA, wluee@eecs.umich.edu

Zeyu Ma NanoScience Technology Center, University of Central Florida,
Orlando, FL 32826, USA; Department of Mechanical, Materials and Aerospace
Engineering, University of Central Florida, Orlando, FL 32826, USA,
zma@mail.ucf.edu

Xin Miao Micro and Nanotechnology Laboratory, Department of Electrical and
Computer Engineering, University of Illinois, Urbana, IL 61801, USA,
xmiao3@illinois.edu

Suman Neupane Department of Physics, Florida International University, Miami,
FL 33199, USA, suman.neupane@fiu.edu

G.P. Peterson Woodruff School of Mechanical Engineering, Georgia Institute
of Technology, Atlanta, GA 303, USA, bud.peterson@gatech.edu

Satish Chandra Rai Advanced Materials Research Institute, University of New
Orleans, New Orleans, LA 70148, USA, scrai@my.uno.edu

Jian Shi Department of Materials Science and Engineering, University
of Wisconsin-Madison, Madison, WI, USA, jshi7@wisc.edu

Ming Su NanoScience Technology Center, University of Central Florida,
Orlando, FL 32826, USA; Department of Mechanical, Materials and Aerospace
Engineering, University of Central Florida, Orlando, FL 32826, USA; School
of Electrical Engineering and Computer Science, University of Central Florida,
Orlando, FL 32826, USA, mingsu@mail.ucf.edu

Limin Tong State Key Laboratory of Modern Optical Instrumentation, Zhejiang
University, Hangzhou 310027, China, phytong@zju.edu.cn

Daniel Vennerberg Department of Materials Science and Engineering, Iowa State
University, Ames, IA 50011, USA, dcv001@iastate.edu

Jun Wang Department of Materials Science and Engineering, Iowa State
University, Ames, IA 50011, USA, junwang@iastate.edu

Kai Wang Advanced Materials Research Institute, University of New Orleans,
New Orleans, LA 70148, USA, kwang1@uno.edu

Xudong Wang Department of Materials Science and Engineering, University
of Wisconsin-Madison, Madison, WI, USA, xudong@enr.wisc.edu

Ye-Liang Wang Institute of Physics, Chinese Academy of Sciences, Beijing 100190, China, ylwang@iphy.ac.cn

Zhong Lin Wang School of Materials Science and Engineering, Georgia Institute of Technology, Atlanta, GA 30332-0245, USA, zlwang@gatech.edu; zhong.wang@mse.gatech.edu

John B. Wiley Department of Chemistry and Advanced Materials Research Institute, University of New Orleans, New Orleans, LA 70148, USA, jwiley@uno.edu

Xukai Xin Department of Materials Science and Engineering, Iowa State University, Ames, IA 50011, USA, xxin@iastate.edu

Qing Yang State Key Laboratory of Modern Optical Instrumentation, Zhejiang University, Hangzhou 310027, China; School of Materials Science and Engineering, Georgia Institute of Technology, Atlanta, GA 30332, USA, qingyang@zju.edu.cn

Yusheng Yang Research Institute of Chemical Defense, Beijing 100191, China, yangyush@public.bta.cn

Zongfu Yu Department of Applied Physics, Stanford University, Stanford, CA 94305, USA, zfyu@stanford.edu

Hai-Gang Zhang Institute of Physics, Chinese Academy of Sciences, Beijing 100190, China, hg Zhang@iphy.ac.cn

Hao Zhang Research Institute of Chemical Defense, Beijing 100191, China, dr.h.zhang@hotmail.com

Minghui Zhang NanoScience Technology Center, University of Central Florida, Orlando, FL 32826, USA, zhangmh@nankai.edu.cn

Weilie Zhou Advanced Materials Research Institute, University of New Orleans, New Orleans, LA 70148, USA, wzhou@uno.edu

Jia Zhu Department of Electrical Engineering, Stanford University, Stanford, CA 94305, USA, jiazhu@stanford.edu

Chapter 1

Building 3D Nanostructured Devices by Self-Assembly

Steve Hu, Jeong-Hyun Cho, and David H. Gracias

1.1 The Pressing Need for 3D Patterned Nanofabrication

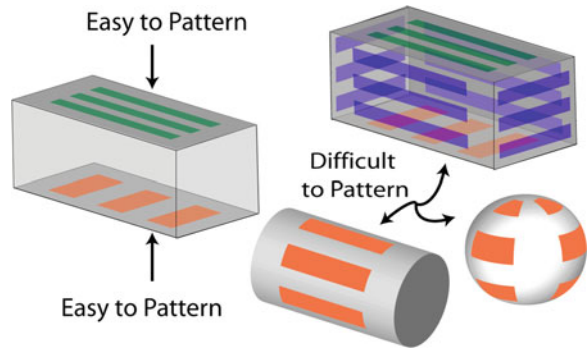
Macroscale engineering is 3D and most structures around us are machined and assembled with a variety of materials that are precisely shaped and patterned. However, while several methodologies exist for precise patterning and assembly at the nanoscale, they can only be enabled in an inherently 2D manner; moreover, many are serial and extremely expensive processes [1–4]. Top-down methods such as particle replication in nonwetting templates (PRINT) [5] have enabled the mass production of nanoparticles, but they tend to have shapes consistent with only a single layer and limited patterning. Hence, there is a pressing need to develop parallel and cost-effective methods for patterning and assembly of 3D nanostructured devices (Fig. 1.1). In this chapter, we discuss methods that focus on the creation of precisely patterned molecular or engineered building blocks that are then driven to assemble themselves into 3D structures using a variety of driving forces. Some of these methods leverage already existing e-beam and imprint lithographic infrastructure by engineering 3D structures from building blocks that are exquisitely patterned in 2D and then subsequently assembled in 3D. We review the challenges associated with self-assembling methodologies with a focus on lithographically defined building blocks and discuss future challenges and prospects.

It is important to clarify at the outset what is meant by a 3D nanostructured device. We characterize one as being composed of either (a) a homogeneous or heterogeneous material composition or (b) structural elements or patterns with a 1–100 nm size scale resolution. Here, one can draw an analogy to macrostructured functional devices such as cars, houses, or planes. An example of a structure with a homogeneous composition on the macroscale is a bare cement wall, while that with a heterogeneous macroscale composition is a cement wall that is interlaid with a glass window and a wooden door with handles. On the microscale, a composite

D.H. Gracias (✉)

Department of Chemical and Biomolecular Engineering, The Johns Hopkins University,
Baltimore, MD 21218, USA
e-mail: dgracias@jhu.edu

Fig. 1.1 Diagram showing the challenges of fabricating 3D patterned nanostructures. Although it is relatively simple to pattern the *top* and *bottom* of a 3D structure, it is very challenging to pattern perpendicular to the plane or on a curved surface



material such as carbon-fiber reinforced steel has a heterogeneous composition, while glass has a homogeneous composition. This analogy suggests that in general, structures and devices with heterogeneous patterning can provide multifunctionality by leveraging functional traits from each element. Nanoscale engineering seeks to facilitate extreme miniaturization at length scales of 1–100 nm, and there is a need to fabricate 3D structures and devices with both homogeneous and heterogeneous composition and with elements whose sizes range from 1 to 100 nm. One vision for the era of miniaturization was beautifully articulated in Richard Feynman’s seminal lecture [6], *There’s plenty of room at the bottom*, where he said, “Consider any machine – for example, an automobile – and ask about the problems of making an infinitesimal machine like it.” At the present time, human engineering is not even close to creating machines like cars at the nanoscale. In fact, while numerous methods have been developed to grow nanostructures such as spherical or branched nanoparticles, nanorods, nanowires, and nanotubes [7–12], these structures have relatively simple shapes with little or no surface patterning.

Multilayer patterning is essential for the construction of circuits, optical elements, energy harvesting tools, and biomedical devices. Recently, alternative unconventional approaches [13] have been pursued to enable this 3D nanofabrication from the bottom-up. The idea has been put forth that there is a need to build complex structures from precursors using a process that mimics biological assembly. This self-assembly approach focuses on bringing together components with pre-programmed interactions to form organized and functional structures. Self-assembling systems typically consist of components such as atoms, molecules, or larger synthetically structured components. The individual parts can typically interact with each other through a variety of chemical or physical forces. Chemical forces include relatively strong interactions such as those facilitated by covalent and ionic bonds or weak interactions such as hydrogen bonds. Physical forces include interactions driven by electrostatic, magnetic, steric, mechanical stress based, or surface tension forces. These components, when brought together, interact through one of the many forces and self-assemble into organized structures. Typically, components are agitated during self-assembly by a variety of means such as Brownian motion, convection, sonication, or physical shaking. This agitation allows components to

explore different orientations and interactions, ultimately enabling stable structures to form within energy minima. Nature is the master of self-assembly, utilizing this approach to create mostly everything from galaxies to humans to seashells and extending all the way down to microorganisms and nanoscale viruses. On closer examination, molecules are self-assembled aggregates of atoms, proteins are self-assembled aggregates of amino acids, and tissues are self-assembled aggregates of cells. It is well known that natural assembly has two distinct self-assembly flavors, namely equilibrium and non-equilibrium self-assemblies. Self-assemblies at equilibrium do not require energy dissipation to maintain their organization; examples include rocks, mountains, or shells. Such assemblies are typically associated with non-living structures. In contrast, non-equilibrium assemblies need to dissipate energy continuously to maintain their organization; examples include microorganisms, humans, and other animals.

Scientists and engineers have long sought to mimic the naturally occurring self-assembly strategy. There are several examples of functional equilibrium self-assembly structures. The stringing together of monomers such as styrene to form synthetic polymers such as polystyrene is a classic example [14]. Synthetic polymers and supramolecules [15] are essentially the chemist's way of engineering self-assemblies using both strong and weak molecular interactions (i.e., chemical bonds). In Section 1.2, we review strategies to enable aggregative self-assembly of 3D nanostructures using molecular linkages and chemical bonds. In Section 1.3, we review strategies for 3D aggregative self-assembly of nanostructures based on physical forces. Section 1.4 focuses on curving, bending, and folding thin films to form 3D curved and polyhedral nanostructures with the possibility of enabling lithographic patterning in all three dimensions.

1.2 Self-Assembly Using Molecular Linkages

Molecular linkages and chemical bonds can be used to direct self-assembly with remarkable specificity and complexity. Through a hierarchy of molecular interactions, naturally occurring molecules are known to form 3D nanoscale functional structures such as viruses [16]. The remarkable experiment by Fraenkel-Conrat and Williams [17] convincingly demonstrated that infectious (active) tobacco mosaic virus (TMV) particles could be self-assembled (reconstituted) from their protein and nucleic acid components. The TMV is an exquisitely patterned nanostructured helix with a helical radius of approximately 4 nm. Presently, the challenge in the creation of synthetic 3D nanostructures composed of molecules lies in understanding how to design the constituent molecular components that will spontaneously form the final structure. Since the number and types of molecular interactions can be large, the rational synthesis of nanostructures using molecules can be arduous. Nevertheless, there have been several elegant demonstrations utilizing molecular linkages such as ligand–receptors, proteins, and nucleic acids. It is also accepted that as compared to self-assembly with physical forces, chemical linkages can provide selective and complex organization [18].

Apart from all molecular assemblies, self-assembly with molecular linkages is also enabled by surface functionalization which serves to modify the surface properties of inorganic nanoparticles so that they may gain some level of specificity in terms of their interactions. The most general form of molecular interaction utilizes ligand–receptor interactions by attaching a ligand molecule to one particle and its complementary receptor molecule to another [19]. Ligand–receptor-based 2D self-assembly has been used in the past for the construction of self-assembled molecular squares [20]. These squares, which are composed of ligand-assisted attached molecules, can incorporate higher order arrangements of 2D structures like diamonds surrounded by smaller squares. Furthermore, functionalization can improve the durability of self-assembled structures since the ligand–receptor attraction is typically enhanced by a conformational fit.

A secondary improvement in functionalization is the ability for the final assembled product to have inherent sensing or actuation capabilities. Since many of the ligands and receptors are key contributors in well-studied biochemical mechanisms, they are capable of sensing. For example, while hydrogen bonding between base pairs in DNA (which will be covered in a later section) can serve as an impetus for self-assembly, aptamer moieties can interact with proteins present in the environment, thereby providing sensing capabilities. Also, many of these ligand–receptor pairs have specific activation and deactivation conditions like temperature or pH, making it possible for the linkages to be made or broken reversibly [18].

It is self-evident that there are a myriad of ligand–receptor combinations that can be chosen to functionalize inorganic particles. For instance, the use of carbon black [21], β -cyclodextrin [22], and methoxysilanes [23] has all been realized for the self-assembly of 3D nanorods and crystals. In this chapter, we will specifically focus on protein (with emphasis on biotin–avidin/biotin–streptavidin) and nucleic acid applications for functionalization since these are the most domineering areas.

1.2.1 Three-Dimensional Self-Assembly Using Protein Linkages

Proteins are ideal for assembling complex nanostructures for many reasons. First, each protein displays a unique conformation in order to ensure specificity, guaranteeing that it will bind strongest when the arrangement and composition of its substrate are correct. Second, proteins can have multiple recognition sites or binding domains, which grants these molecules with an inherent 3D ligand-binding capability. Finally, proteins are easily modified; their structures can be genetically edited [24] to omit or add certain binding subunits.

Several 3D nanostructures composed solely of protein constituents have been demonstrated. The shapes range from nanofibers [25] to nanotubes [26] to protein cages [27] and can be designed at a high level of specificity. Typically, the required proteins are chosen from the Protein Data Bank, which stores the structural information of many characterized proteins. This choice allows for the selection of structural or binding motifs like a terminal α -helix thereby enabling greater control

over binding sites. After the systematic selection of these proteins, it is also possible to modify their binding characteristics by varying conditions such as pH [25] or engineering specific regions [28].

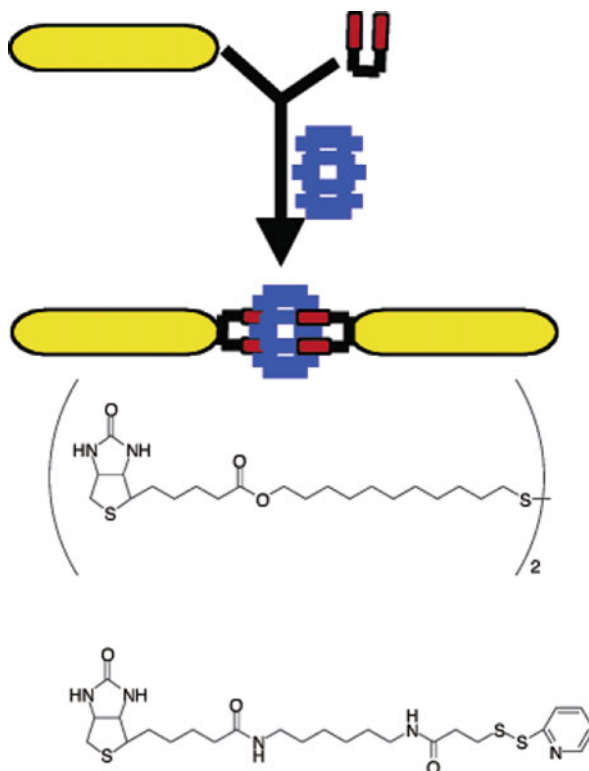
Since proteins assemble with high specificity, they can be used in conjunction with nanoparticles through surface functionalization. Functionalization of inorganic particles using proteins can be done using multiple strategies. For example, nanoparticles composed of noble metals such as gold can be first thiolated and subsequently cross-linked with a desired protein's amine group through the use of 1-ethyl-3-(3-dimethylaminopropyl)-carbodiimide/*N*-hydroxysuccinimide (EDC/NHS) reaction scheme [29]. Other charged inorganic nanoparticles like silica can be functionalized by using proteins with charged amino acid residues like lysine, a method which has been applied to form shapes like hollow spheres [30].

One very popular method of functionalizing inorganic molecules is achieved by using the proteins avidin or streptavidin in conjunction with the ligand biotin, a coenzyme. Both avidin and streptavidin are tetrameric proteins which contain four identical binding sites to biotin. The binding strength of biotin to its protein receptor site is extremely strong; it is comparable to that of a covalent bond with a binding constant, K_a , of 1×10^{15} M [31]. With such a high binding strength, the biotin-avidin pair works well in self-assembly, since covalently linked structures are quite stable. Having multiple sites for a ligand can also introduce hierarchical capabilities, where a primary scaffolding molecule can serve to "host" a number of surrounding molecules during assembly.

Let us examine a biotin-streptavidin linkage that has proven successful in 3D self-assembly of inorganic nanostructures. Ferritin is a protein-metal conjugate that is made of a protein shell which encapsulates a ferric oxide core. For biotinylation, ferritin can use its external lysine residues to bind up to 60–70 biotin molecules by a nucleophilic reaction [32]. Once the ferritin has been biotinylated, streptavidin can be added at varying ratios in order to provide adequate streptavidin for cross-linking. However, the streptavidin concentration cannot be too high or it may prevent biotinylated particles from linking to the same streptavidin protein. In one study, this optimal ratio was measured to be approximately one biotinylated ferritin to six streptavidin [32]. To build a 3D nanostructure, biotinylated ferritin can be linked to a primary structure such as a carbon nanotube [33] through hydrophobic interactions to enable the self-assembly of a multilayer nanotube composed of different material layers. An additional concentric layer of a different inorganic metal could also be linked onto this ferritin shell by adding other biotinylated metals.

Another example of controlled self-assembly using biotin-streptavidin can be exemplified through the end-to-end binding of gold nanorods in an experiment performed by Caswell et al. [34]. Biotinylation in this case was achieved using biotin disulfides, which can form disulfide linkages to gold surfaces. Since the nanorods were controllably formed using a cetyltrimethylammonium bromide (CTAB) surfactant, functionalization was hypothesized to only form at the ends of the rods where CTAB was not present. Therefore, the addition of streptavidin would only self-assemble the nanorods end to end instead of connecting them at the sides (Fig. 1.2).

Fig. 1.2 Scheme showing the assembly of gold nanorods (*golden ovals*) by surface functionalization with the biotin disulfide (*red*), and subsequent addition of streptavidin (*blue*) to produce aggregates of nanorods. The chemical structures of the two biotin disulfides are also shown, homemade (*top*) and commercial EZ-Link Biotin-HPDP (*bottom*). Reprinted with permission from [34]. Copyright 2003 American Chemical Society



With the many available methods to biotinylate different inorganic particles, it is possible to create complicated self-assembled structures. In addition, direct control over the region which is biotinylated and the concentration of streptavidin or avidin grants control over the complexity of the assembled structure. Therefore, by using this simple ligand–protein construct, we can expand the possibilities in constructing devices with differing shapes and metal compositions.

1.2.2 Three-Dimensional Self-Assembly with DNA Linkages

Another exciting field enabling the creation of 3D nanostructures is DNA self-assembly. Just like proteins have many benefits for their use in self-assembly, DNA also has significant advantages for its use. DNA is extremely well understood in terms of base pairing and crystallographic structure, making it very predictable and programmable when used as a template for self-assembly [35]. From basic biology, we know that adenine will preferentially bind to thymine, and cytosine will preferentially bind to guanine by hydrogen bonding. Therefore, the assembly of DNA is already quite intuitive from a scientific standpoint.

DNA self-assembly is utilized in two categories for 3D self-assembly: the use of DNA motifs to create origami-like structures made of pure DNA [36] and the use of DNA as a nanoparticle scaffold by functionalization for assembly [37]. The latter portion of DNA technology is very similar to that of protein self-assembly, where the binding originates from specific linkers. Both schemes have brought much potential to enable the creation of devices that can be applied as biosensors, nanophotonic devices, nanoelectric devices [38], and drug delivery vehicles [39].

The folding of 3D DNA structures began with the work of Nadrian Seeman. In 1991, Seeman was able to synthesize a cube solely made from ligated DNA strands by using sticky ends as a linking device [40]. Each vertex of the cube had to be meticulously connected in order to form the final structure, making it a very difficult, low-yield task. Instead, researchers explored other options by starting from stable DNA structures to make 3D nanostructures.

One simple structure is a DNA junction, which is a point where multiple strands of DNA meet via a complementary linkage or through the use of a tris-linker [41]. The junctions allow one to form a DNA folding template, where the structure is already connected and only requires binding intramolecular regions to gain 3D architecture. In one method, a 1669 nt single strand of DNA with multiple junctions was designed with complementary terminal branches. With the assistance of smaller linker sequences, the strand could form crossovers in the center which brought the terminal branches together to form a 3D octahedron [42].

The discovery of the rigidity of triangular-based DNA structures lent credence to the notion that DNA motifs could be used for complicated 3D assembly. The triangular-based structures include trisoligonucleotides (three strands joined by a center tris-linker) and tetrahedrons. The trisoligonucleotides were shown to be able to produce a dodecahedron by utilizing complementary strand sequences as connectors and the center as a vertex [41]. Tetrahedrons are especially viable due to their simple construction protocol; it has been demonstrated that four equal oligonucleotides with complementary regions for each other could be annealed and ligated to self-assemble a DNA tetrahedron with high yield [43]. The tetrahedrons can then be used for advanced functions like protein encapsulation [44] and structural (i.e., bending, twisting) modifications by activating hairpin sequences [39]. In addition, by using a DNA linking strand, it is possible to add a higher level of complexity by assembling multiple tetrahedral DNA motifs [43].

One DNA self-assembly experiment involved the use of DNA “tiles,” which are star motifs that can contain multiple symmetric points. A three-point star tile contains a long central strand, three medium strands, three short exterior strands, and three central loops [45]. Each point’s end contains a sticky end to be able to latch onto the points of other identical tiles. It was discovered that the length of the central loops allowed for control over the self-assembly of the tiles. Lengthening the loop meant the tile had more curving flexibility and could form 3D shapes more readily through exposing the sticky ends. This, in conjunction with a relatively low DNA tile concentration to increase the chance of connected structures to interact, allowed for the self-assembly of tetrahedral-shaped structures (Fig. 1.3). By adding more DNA tiles and shortening the loop to reduce strand bending, dodecahedrons

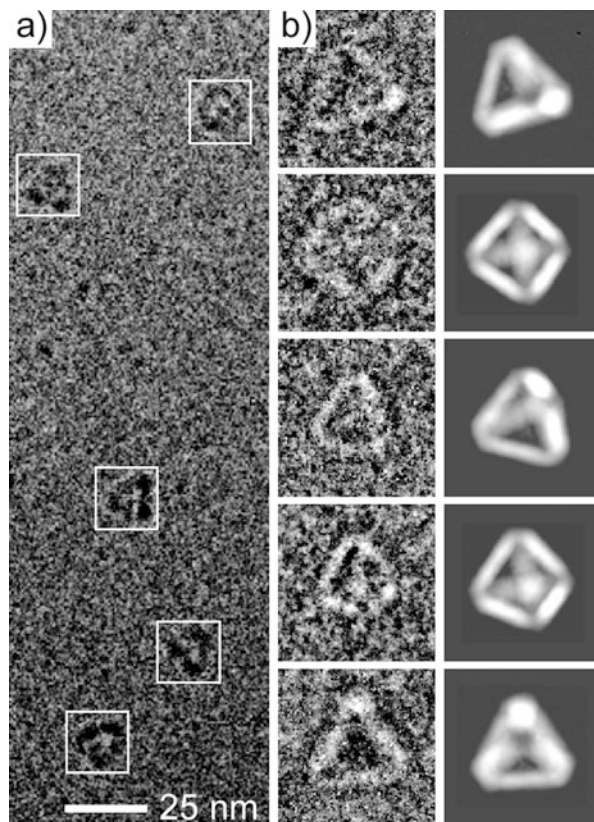
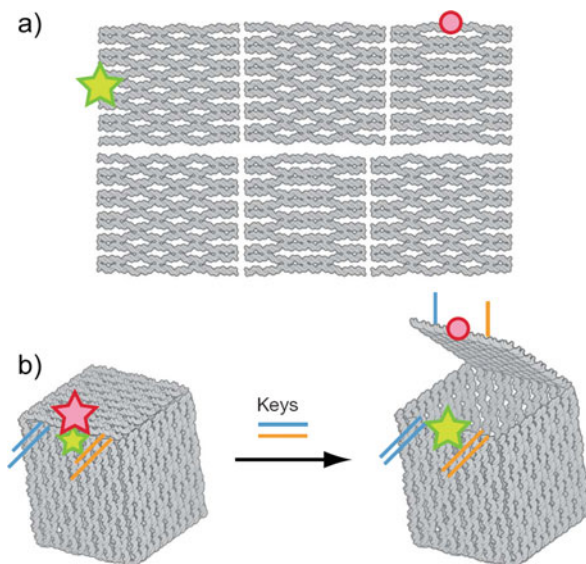


Fig. 1.3 Characterization of the DNA tetrahedron by DLS, AFM, and cryo-EM. **(a)** A representative cryo-EM image. *White boxes* indicate the DNA particles. **(b)** Raw cryo-EM images of individual particles and the corresponding projections of the DNA tetrahedron 3D structure reconstructed from the cryo-EM images. These particles are selected from different image frames to represent views at different orientations. Reprinted with permission from [45]. Copyright 2008 Macmillan Publishers Ltd (Nature Publishing Group)

and buckyballs [45] were formed, possibly arising due to the smaller curvatures of these larger 3D structures. The same phenomenon is observed in five-point stars as well, where longer loops and lower DNA concentrations are found to produce icosahedrons [46].

To simplify DNA folding, a later technique called DNA origami [47] was developed by Paul Rothemund, which involved the use of a long strand of DNA as a large scaffold with hundreds of specific “staple” DNA strands to form crossovers which tighten or bend the scaffold. These staple strands are meticulously programmed to form desired crossovers at repeated turn length intervals through the use of a DNA software system that can pattern the complementary sequences. By using this technology, one can form DNA templates for folding 3D nanostructures with great precision. One experiment displayed the folding of a nanoscale DNA box with a

Fig. 1.4 Programmed opening of the box lid. Illustrations of the unlinked faces of the box (a) and the controlled opening of the box lid (b). The emission from the Cy5 and Cy3 fluorophores is marked with *red* and *green* stars, respectively. Loss of emission from Cy5 is denoted by a *red circle* and the independent lock–key systems are indicated in *blue* and *orange*. Reprinted with permission from [48]. Copyright 2009 Macmillan Publishers Ltd (Nature Publishing Group)



controllable lid [48] through the use of DNA origami by starting with a linked template of six DNA squares. The staple strands assisted in the folding of the squares to form a cubic structure with specific sticky ends to grant complementary oligonucleotide “keys” access to open the box with a conformational change (Fig. 1.4).

DNA, like biotin–streptavidin, can also be used for the self-assembly of inorganic particles through functionalization. There are multiple methods used to tether a strand of DNA to an inorganic nanoparticle. Some involve using charge interactions [49] since DNA is negatively charged, while some metals have cationic properties. These interactions can allow DNA to become a template on which metal nanoparticles may aggregate [50]. Another common functionalizing technique uses gold–thiol linkages to the thiolate DNA [38, 51, 52]. Like the arrangement of protein-linked nanoparticles, DNA-functionalized nanoparticles have high specificity since they will only bind to complementary strands.

Binding specificity was demonstrated through an experiment involving different sized gold particles (diameters of 8 and 31 nm) that were functionalized with complementary oligonucleotides [53]. The particles self-assembled to form a “satellite” structure, which is distinguished by a large central particle surrounded by multiple linked smaller particles (Fig. 1.5). When the oligonucleotides were omitted from these particles, self-assembly did not yield any organized structure [53]. This self-assembly has been applied to not only nanoparticles but also nanostructures like gold nanorods [54]. Added complexity is also possible through the use of biotinylated oligonucleotides that are functionalized onto nanoparticles [55]; streptavidin can be added after hybridization to induce stepwise assembly.

DNA self-assembly is one of the best understood molecular technique today simply because of our ability to manipulate DNA easily. The biological and materials

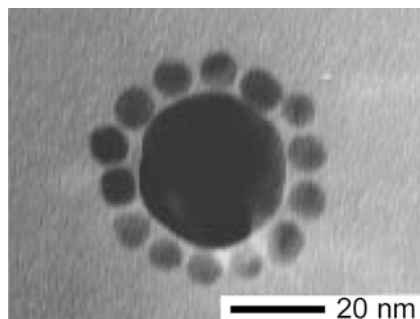


Fig. 1.5 TEM image of the binary nanoparticle network materials supported on holey carbon grids. A nanoparticle satellite structure obtained from the reaction involving 120:1 modified 8 nm particles:modified 31 nm particles and linking oligonucleotides. Reprinted with permission from [53]. Copyright 1998 American Chemical Society

device applications are not trivial, and additional functions can be made with ease. There has been some work to date on RNA self-assembly involving magnesium-mediated RNA and its receptor loop RNA to produce self-assembled gold nanowires [56]. Functionalization occurs through the use of DNA–RNA complementary binding regions secondary to a primary DNA thiol linkage to gold.

1.3 Three-Dimensional Self-Assembly Using Physical Forces

While self-assembly with molecular linkages provides remarkable versatility and specificity in terms of the kinds of interactions that can be engineered, many of these linkages fall apart when the structures are dehydrated or heated. Hence, there is a need to explore the assembly of structures using physical forces. Moreover, devices with magnetic, photonic, or electrical properties often require the incorporation of inorganic components such as metallic or semiconducting materials [57]. There is often a need to organize metallic and inorganic components with nanoscale precision to enable functional 3D nanostructured devices. In this sense, it is already established that self-assembly provides an attractive route to fabricate nanoscale structures [58].

Three-dimensional methods build upon conventional 2D self-assembly methods. The 2D methods typically form arrays or monolayers of nanostructures. Most of these 2D structures are formed by utilizing a physical force to coax nanoparticles into their desired places. For example, the use of surface interactions in Langmuir–Blodgett films at the air–liquid interface can be applied to generate the self-assembly of a monolayer of nanoscale particles [59] and even nanorods [60]. Other methods have involved evaporating thin liquid films over a solid support [61–63]. The 2D self-assembly of an array or monolayer of nanoscale particles by evaporation is driven by capillary forces that pull particles together during removal of the liquid.

After evaporation, the particles are held together by van der Waals or dispersion forces.

To move into the third dimension, one approach focuses on shape control, namely, by synthesizing colloids with a 3D morphology. These inorganic particles are fabricated in solvents with varying pH, concentration, temperature, and voltage; the resulting nanostructures have complex 3D morphologies and resemble flowers, helices, discs, and hollow boxes [64–66]. Another example involves the self-assembly of CdSe quantum dot superlattices by a nucleation-caused crystallization in solution; the lattices are then held together by intermolecular forces [67]. Dipole–dipole interactions are also utilized to create 3D rod-like structures with anisotropic control using a surfactant [68].

The use of physical templates to shape the overall self-assembly has enabled control over both the arrangement and the interactions among constituent particles. Templates can also be structured using electron beam lithography, imprint lithography, particle track etching, or by anodization. Self-assembly of a hexagonal closed packed or face-centered cubic silica colloidal crystal has been demonstrated using a uniform template; small defects in the template reflect small defects in the crystal [69]. By constricting the volume of the template on the nanoscale, one can produce a wide range of structures [70] (Fig. 1.6). Linked templates are also used, which involve a chemically functionalized template to bind to a specific inorganic compound. This helps to produce a hierarchical self-assembly [71], where inorganic molecules can link onto an initial self-assembled structure and then build upon it to form complicated structures such as sieves [72]. The linked template method has been mastered to the extent to which even a nanoscale painting by Picasso [73] has been replicated using colloidal gold!

Van der Waals or dispersion forces are widely used to hold together nanostructured organizations after self-assembly. However, it should be noted that this force is weak, and the nanostructures can often be disrupted by sonication. For example, the cubic assemblies shown in Fig. 1.7 were formed by self-assembly of selectively functionalized hydrophobic units in water. Here, selective functionalization of different faces of silver (Ag) cubes was achieved using hydrophobic (octadecanethiol) and hydrophilic (mercaptohexadecanoic acid) thiols. Selective functionalization results in the formation of linear chains and closed packed crystals; however, the units are held together only by weak van der Waals forces [74]. Similar assemblies were demonstrated using nanowires with amphiphilic segments [75] and were even observed during dissolution of the templates (Fig. 1.8a) [76]. These 3D nanostructures, although self-assembled in impressive 3D geometries, would fall apart upon sonication. Self-assembly with segmented nanowires provides some specificity in the interactions by the inclusion of hydrophobic, hydrophilic [75], or magnetic (Fig. 1.8c–d) segments [77].

Permanent bonding of units after assembly can be achieved using surface tension-based assembly with liquid drops that solidify on cooling or cross-linking. This approach draws inspiration from mesoscale self-assembly approaches [78–81] to permanently bond nanoscale assemblies using adhesives [82] (Fig. 1.8e–f) or solder [83]. These bonded assemblies survive sonication. Additionally, selective patterning

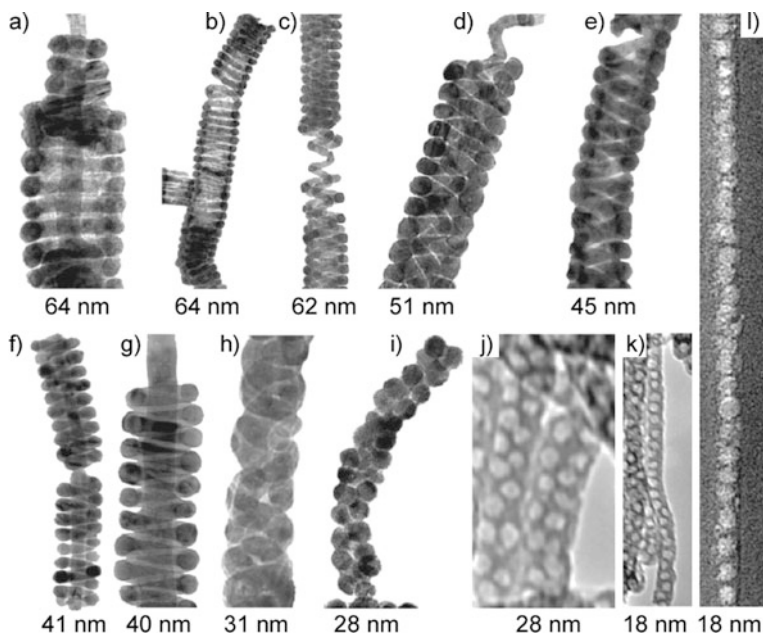


Fig. 1.6 Representative TEM images of mesostructures formed inside alumina nanochannels with differing confinement dimensions. The confining nanochannel diameter is indicated underneath each image. (a–i) Silver inverted mesostructures prepared by backfilling the confined mesoporous silica; (j–k) free-standing mesoporous silica fibers; (i) mesoporous silica embedded inside the alumina nanochannels obtained using a focused ion beam for sample preparation. The structures are (a) three-layer stacked *doughnuts*; (b) S-helix; (c) core–shell D-helix, in which the core and the shell are both S-helix; (d) core–shell triple helix, in which the shell is a D-helix and the core is an S-helix; (e) D-helix; (f, g) S-helix with a straight core channel; (h) D-helix; (i, j) inverted *peapod* structure with two lines of spherical cages packed along the long axis of the alumina nanochannel; (k, l) inverted *peapod* with one line of cages. Reprinted with permission from [70]. Copyright 2007 Macmillan Publishers Ltd (Nature Publishing Group)

of segments of nanowires with self-assembled monolayers enables specific bonding of these segments with hydrophobic monomers that can be subsequently cross-linked (Fig. 1.8f).

1.4 Three-Dimensional Patterned Nanofabrication by Curving and Bending Nanostructures

One attractive strategy to enable patterning in 3D is to leverage precise 2D nanofabrication paradigms to create units that are then rotated or bent into the third dimension. The forces required to achieve this curving or bending can be derived from several mechanisms including thin film stresses, magnetism, pneumatics, swelling, and surface tension [84]. Most of the prior research involving the above mechanisms has been limited to the microscale. Here, we focus on two mechanisms